A Theoretical Investigation on Kinetics, Mechanism, and Thermochemistry of the Gas-Phase Reactions of Methyl Fluoroacetate with OH Radicals and Fate of Alkoxy Radical

ARTICLE *in* THE JOURNAL OF PHYSICAL CHEMISTRY A · AUGUST 2014

Impact Factor: 2.69 · DOI: 10.1021/jp5032042 · Source: PubMed

2 AUTHORS:

Bhupesh Kumar Mishra
D. N. Government College, Itanagar, Arunacha…
45 PUBLICATIONS **279** CITATIONS
SEE PROFILE

Ramesh Chandra
Indian Institute of Technology Roorkee
186 PUBLICATIONS **1,543** CITATIONS
SEE PROFILE

THE JOURNAL OF PHYSICAL CHEMISTRY A

Article

pubs.acs.org/JPCA

A Theoretical Investigation on Kinetics, Mechanism, and Thermochemistry of the Gas-Phase Reactions of Methyl Fluoroacetate with OH Radicals and Fate of Alkoxy Radical

Bhupesh Kumar Mishra* and Ramesh Chandra Deka*

Department of Chemical Sciences, Tezpur University, Napaam, Tezpur, Assam-784 028, India

Supporting Information

ABSTRACT: We theoretically investigated OH-initiated hydrogen abstraction reactions of methyl fluoroacetate (MFA) $CH_2FC(O)OCH_3$ at the MPWB1K level of theory in conjunction with the 6-31+G(d,p) basis set. Thermodynamic and kinetic data are computed using the comparatively accurate G2(MP2) method. Two most stable conformers of MFA are identified, and the energy difference between them is found to be only 0.32 kcal mol^{-1}. Both of them are considered for rate coefficient calculations, and the contribution from each of the conformers is found to be quite significant. We propose an indirect mechanism due to validation of pre- and post-reactive complexes. The rate parameters are determined using canonical transition state theory and energetics at the G2(MP2) level. The temperature dependence of the rate constant can be described by the Arrhenius expressions: $k = 8.79 \times 10^{-13} \exp[(-377.27 \pm 64)/T]$ cm^3 $molecule^{-1}$ s^{-1} over a temperature range of 250−450 K. The $\Delta_f H°_{298}$ for $CH_2FC(O)OCH_3$, $CH_2FC(O)OC^{\bullet}H_2$, and $C^{\bullet}HFC(O)OCH_3$ are also computed using an isodesmic procedure. The OH-driven atmospheric lifetime of MFA was estimated to be 24 days. A mechanistic study to shed light on the atmospheric degradation and the sole fate for the consumption of $CH_2FC(O)OCH_2O^{\bullet}$ radical has also been reported.

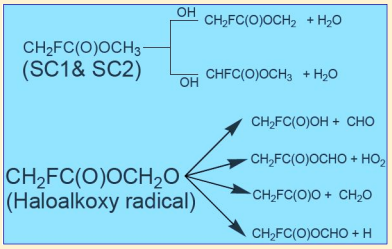

INTRODUCTION

Due to the detrimental effect of chlorofluorocarbons (CFCs) toward the ozone layer,[1,2] much attention has been paid in past decades to find its substitute. Recently, hydrofluoroethers (HFEs) are widely used as a third generation alternative to CFCs in industrial applications.[3−5] Once released into the atmosphere, HFEs undergo OH- and Cl-initiated oxidation leading to the formation of fluorinated esters (FESs) as main degradation products.[6−8] For instance, the perfluorobutyl formate n-$C_4F_9OC(O)H$ is a near-unity product of the degradation of n-HFE-7100 (n-$C_4F_9OCH_3$).[9,10] FESs contain C−H bonds in their molecular structure and are removed from the troposphere mainly by reactions with OH radicals.[11] Recent studies have revealed that atmospheric oxidation of FESs leads to the formation of trifluoroacetic acid (TFA) and COF_2.[12,13] Extensive consideration has been paid in recent years to perform experimental studies on the decomposition kinetics of FESs.[13−17] In 2007, Blanco and Teruel[14] performed a kinetic study on the OH-initiated hydrogen abstraction channel for four fluoroacetates, namely, methyl trifluoroacetate, ethyl trifluoroacetate, methyl difluoroacetate, and 2,2,2-trifluoroethyl 2,2,2-trifluoroacetate, at (296 ± 2) K using the relative technique. Subsequently, Blanco et al.[15] reported the rate constant for Cl-initiated oxidation of fluoroacetates at (298 ± 2) K using in situ FTIR spectroscopy. Recently, the OH radical initiated atmospheric degradation of trifluoroethyl butyrate has been reported by Blanco et al.[17] The Cl-initiated atmospheric degradation mechanism and reactivity of $CF_3C(O)OCH_2CF_3$ have been investigated by Blanco et al.[12] Considerable theoretical studies on the degradation mechanism of FESs were performed in our group.[18−21] Recently, Singh et al.[22] performed a mechanistic and kinetic study on OH-initiated abstraction reactions of methyl difluoroacetate ($CF_2HCOOCH_3$). Bravo et al.[23] have developed a methodology to predict radiative efficiencies (REs) and global warming potentials (GWPs) for fluoroalkyl formates. Due to its greater toxicity and pharmacological properties,[24] MFA has been used a starting material for producing tosufloxacin, 5-fluorouracil, floxuridine, 5-fluoro-4-hydroxylpyrimidine, and so on.

In the present study, the gas-phase hydrogen abstraction reactions between MFA and OH radicals are investigated by means of theoretical tools for the first time. Preliminary observation reveals that the three hydrogen atoms in the $-CH_3$ group are not equivalent. So, two reaction channels from $-CH_3$ and one reaction channel from $-CH_2F$ groups are considered in detailed for $CH_2FC(O)OCH_3$ + OH reactions as given below:

$$CH_2FC(O)OCH_3 + OH \rightarrow CH_2FC(O)OC^{\bullet}H_2 + H_2O \quad \text{(R1a and R1b)}$$

$$CH_2FC(O)OCH_3 + OH \rightarrow C^{\bullet}HFC(O)OCH_3 + H_2O \quad \text{(R2)}$$

Two stable conformers (SC1 and SC2) are identified for MFA. The energy difference is found to be only 0.32 and 0.21 kcal mol^{-1} at the G2(MP2) and MPWB1K/6-31+G(d,p) levels,

Received: April 1, 2014
Revised: August 28, 2014
Published: August 29, 2014

dx.doi.org/10.1021/jp5032042 | J. Phys. Chem. A 2014, 118, 8779−8786

respectively which implies that both of them may have contribution to the title reaction. Moreover, the standard enthalpy of formation ($\Delta_f H^\circ_{298}$) for $CH_2FC(O)OCH_3$ and radicals $CH_2FC(O)OC^\bullet H_2$ and $C^\bullet HFC(O)OCH_3$ are computed using isodesmic work reactions for the first time. The reactivity of HFEs toward atmospheric oxidants has been correlated with the C−H bond strength, and their rate coefficients are derived.[25] Thus, we also estimate bond dissociation energies of C−H bonds in MFA.

The mechanism and different pathways which lead to $CH_2FC(O)OCH_2O^\bullet$ radical by OH-initiated oxidation of MFA are shown in Scheme 1. Blanco et al.[13] experimentally

Scheme 1. Tropospheric Degradation of MFA

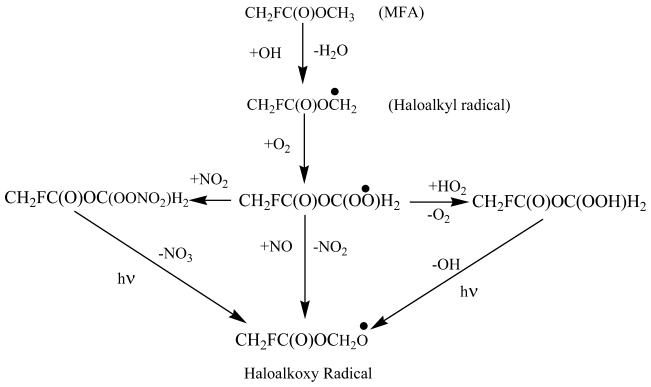

investigated Cl-initiated oxidation of MDFA at (296 ± 2) K and atmospheric pressure (760 Torr). Two competitive processes (α-ester rearrangement and oxidation with O_2) for fluoroalkoxy radical were rationalized. Recently, numerous efforts have been paid to study the reactivity of alkoxy radicals.[26−29] Thus, four plausible pathways are considered during the present study for decomposition of alkoxy radical that involve α-ester rearrangement, oxidation process, and thermal decomposition (C−O and C−H bond scission) as follows:

$$CH_2FC(O)OCH_2O^\bullet \rightarrow CH_2FC(O)OH + CHO^\bullet \quad (R3)$$

$$+O_2 \rightarrow CH_2FC(O)OC(O)H + HO^\bullet_2 \quad (R4)$$

$$\rightarrow CH_2FC(O)O^\bullet + CH_2O^\bullet \quad (R5)$$

$$\rightarrow CH_2FC(O)OC(O)H + H \quad (R6)$$

COMPUTATIONAL METHODS

The structure optimization of all stationary points involved in the hydrogen abstraction reactions (reactants, reaction complexes, transition states, product complexes, and products) was performed by using the meta-GGA functional MPWB1K, as developed by Truhlar and co-workers[30] with use of 6-31+G(d,p) basis set. In recent studies[32−34] it has been reported that this method (MPWB1K/6-31+G(d,p)) can be applied effectively to predict transition state geometries, vibrational frequencies, and thermochemical and kinetics data. On the basis of optimized geometries, the vibrational frequency calculations were performed to determine whether a stationary point was either a minimum with all positive frequencies (NIMAG = 0) or a transition state with only one imaginary frequency (NIMAG = 1) and to correct energies for zero-point and thermal contributions at 298 K. The intrinsic reaction coordinate (IRC) calculations[35] were performed at the same level of theory to confirm whether the transition state connects the desired reactants and products. In order to refine reaction enthalpies and potential energy surface, the single-point energy calculations were performed at G2(MP2)[36] using optimized geometries at the MPWB1K level. Our previous studies[31,37−39] reveal that this procedure, i.e., the use of the G2(MP2)//MPWB1K approach, properly describes the energetics and kinetics features for hydrogen abstraction reactions and decomposition reactions. All electronic structure calculations are performed with the GAUSSIAN 09 program package.[40] As we mentioned, the two most stable conformers (SC1 and SC2) of $CH_2FC(O)OCH_3$ are very close in energy. Therefore, the thermodynamic quantity (Q) for conformers SC1 and SC2 is computed using the Boltzmann distribution equation[41] as given in eq 1,

$$Q = W_{SC1}\cdot Q_{SC1} + W_{SC2}\cdot Q_{SC2} \quad (1)$$

where W_{SC1} and W_{SC2} are statistical weight factors of conformers SC1 and SC2, respectively.

RESULTS AND DISCUSSION

On structural optimization of MFA two minima (SC1 and SC2) were identified by rotating about the C1−F1 bond relative to the F−C−C−O backbone. The F1−C1−C2−O2 dihedral angle is 0.0° in the SC1 conformer; whereas the same is 179.98° in the SC2 conformer. This is in accord with the conformational analyses of Abraham et al.[42] and Sahnoun et al.[43] by means of theoretical tools. Their structures are shown in Figure 1. It can be seen that our calculated geometrical parameters for MFA agree well with that reported by Abraham et al.[42] The OH radicals can attack from two sites, namely, the $-CH_3$ and $-CH_2F$ groups of MFA. Our calculations reveal that the three hydrogens in the $-CH_3$ group are not equivalent and two channels (R1a and R1b) are feasible from the $-CH_3$ group. Therefore, three channels are considered for both conformers and six transition states (TS_{a1}, TS_{b1}, TS_{21}, TS_{a2}, TS_{b2}, and TS_{22}) are located for reaction channels (R1−R2). We also notice the existence of hydrogen-bonded pre- and postreactive complexes (RCs and PCs) for both reaction channels from IRC calculations. These prereactive complexes, having energies lower than those of reactants, are stabilized by multiple hydrogen bonding interactions as shown in Figure S1 in the Supporting Information. At the same time, the postreactive complexes (PCs) are stabilized by hydrogen bond attractive interaction with C−H···O and O−H···F bonds, as shown in Figure S1 in the Supporting Information. Thus, we propose that both reaction channels proceed via indirect mechanisms. The calculated reaction enthalpies $\Delta_r H^\circ_{298}$ of title reactions at both levels are recorded in Table 1, which shows that both reactions are exothermic in nature. The structural parameters for all the species are depicted in Figure 1. Moreover, our calculated structural parameters for MFA given in Figure 1 are consistent with the values as reported by Abraham et al.[42] At the MPWB1K level, for TS_{a1}, TS_{b1}, TS_{21}, TS_{a2}, TS_{b2}, and TS_{22}, the breaking C−H bonds are found to be elongated all in a range of 9.67−12.44% compared to the C−H bond length in isolated $CH_2FC(O)OCH_3$; whereas the forming O···H bond length is longer by 33.89 to 39.45% than the O−H bond length in H_2O. It indicates that the reactions may proceed via early transition states. The results of frequency calculations for all the stationary points are recorded in Table S1 in Supporting

dx.doi.org/10.1021/jp5032042 | J. Phys. Chem. A 2014, 118, 8779−8786

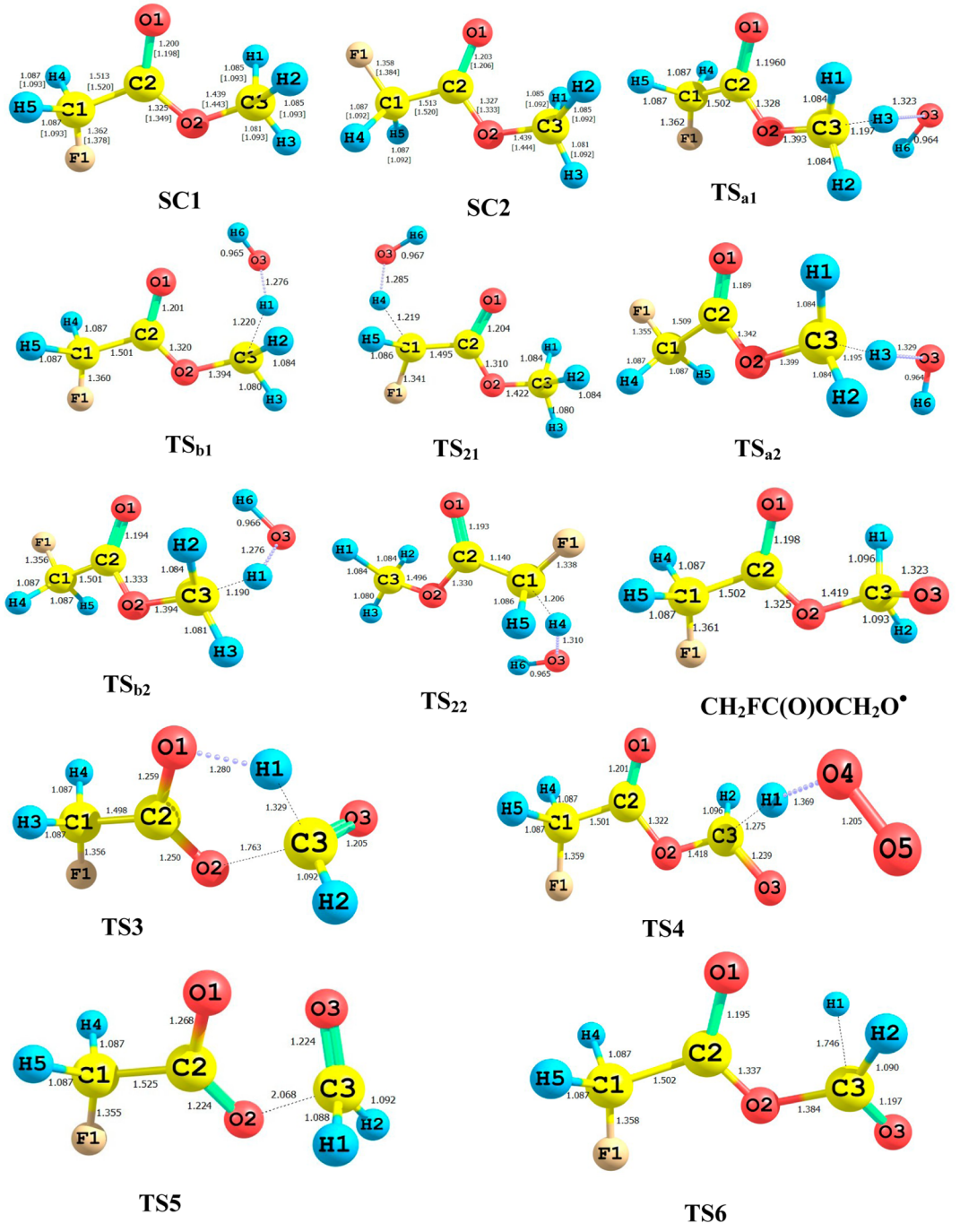

Figure 1. Optimized geometries of reactants and transition states at the MPWB1K/6-31+G(d,p) level. The values given in parentheses are taken from ref 42.

Table 1. Reaction Enthalpies for the H Abstraction Reaction Channels of MFA with OH Radicals Calculated at the G2(MP2) and MPWB1K/6-31+G(d,p) Levels of Theory[a]

conformer	reaction channels	G2(MP2)	MPWB1K
SC1	R1	−18.04	−15.31
	R2	−16.65	−14.70
SC2	R1	−17.72	−15.10
	R2	−16.33	−14.49
	wt-av R1	−17.91	−15.21
	wt-av R2	−16.52	−14.60

[a]All values are in kcal mol^{-1}.

Information, which reveals that the values of imaginary frequencies for TS$_{a1}$, TS$_{b1}$, TS$_{21}$, TS$_{a2}$, TS$_{b2}$, and TS$_{22}$ are found to be 1160i, 1502i, 1523i, 1105i, 1498i, and 1316i cm^{-1}, respectively, corresponding to the reaction coordinate. Intrinsic reaction calculations (IRC)[35] further confirm that each transition state structure connects the desired reactants and product.

The associated energy barriers including ZPE correction for species calculated at both levels are recorded in Table S2 in the Supporting Information. The G2(MP2) calculated barrier heights for TS$_{a1}$ and TS$_{b1}$ (reaction R1) are 4.54 and 1.86 kcal mol^{-1}, respectively. The same from MPWB1K results amount to 3.61 and 1.30 kcal mol^{-1}. Similarly, the calculated

dx.doi.org/10.1021/jp5032042 | J. Phys. Chem. A 2014, 118, 8779−8786

barrier heights for reaction R2 (TS_{21}) are 2.62 and 2.27 kcal mol^{-1} at the G2(MP2) and MPWB1K levels, respectively. Similar calculations performed for transition states TS_{a2}, TS_{b2}, and TS_{22} for conformer SC2 yield 4.75, 1.94, and 3.34 kcal mol^{-1} at the G2(MP2) level and 3.87, 1.34, and 2.90 kcal mol^{-1} at the MPWB1K level, respectively. Thus, energetic calculations reveal that the $-CH_3$ group (TS_{b1} and TS_{b2}) of MFA is more favorable than the $-CH_2F$ group toward hydrogen abstraction reactions.

Moreover, due to scarcity of any literature values, we compared our results with a recent theoretical study by Singh et al.[22] on a similar species. For that purpose, we have located the two transition states (TS7 and TS8) from $-CF_2H$ and $-CH_3$ sites of the $CF_2HC(O)OCH_3$ molecule at the same level of theory. The optimized geometries of $CF_2HC(O)OCH_3$, TS7, and TS8 are shown in Figure S1 in the Supporting Information. Using these geometries energetic calculations were performed at the G2(MP2) level, and relative energies are found to be 3.60 and 1.85 kcal mol^{-1}, respectively. It can be seen that our calculated barrier heights agree well with the reported values of 3.19 and 2.30 kcal mol^{-1} at the G3B3//MPWB1K/6-31+G(d,p) level by Singh et al.[22] Moreover, an intensive ab initio calculation performed by Yang et al.[44] for the $-CH_3$ site of $CH_3C(O)OCH_3$ amounts to 4.33 kcal mol^{-1} at the QCISDT//MP2 level. The values obtained in present study at the G2(MP2)//MPWB1K level for the same site of the $CH_2FC(O)OCH_3$ molecule are consistent with that reported by Yang et al.[44] Since our barrier heights agree well with the previous results, we can conclude that the procedure taken during the course of the present investigation yields reliable results.

The lowering of barrier heights in the case of $CH_3C(O)OCH_3$ is expected due to replacement of the more electronegative F atom in $CH_2FC(O)OCH_3$ by the H atom in $CH_3C(O)OCH_3$, which can be analyzed in terms of change in electron density distribution. Gas-phase reaction profiles for the SC1/SC2 + OH is shown in the Supporting Information (Figures S2 and S3). The energy of reactants is set to be zero as a reference. The results reveal that hydrogen abstraction by OH radicals from the $-CH_3$ group of MFA is more facile than that from the $-CH_2F$ group. This finding agrees well with the observation made by Singh et al.[22] for a similar species, $CF_2HC(O)OCH_3$ + OH reactions. This conclusion is further confirmed by bond dissociation energy calculations.

The $\Delta_fH^\circ_{298}$ for MFA and the radicals $CH_2FC(O)OC^\bullet H_2$ and $C^\bullet HFC(O)OCH_3$ are computed for the first time using an isodesmic reaction approach. We have used work reactions R7–R9 to compute $\Delta_fH^\circ_{298}$ for MFA.

$$CH_2FC(O)OCH_3 + CH_3CH_3 + CH_3F \rightarrow CH_3COCH_3 + CH_3OCH_3 + CH_2F_2 \quad (R7)$$

$$CH_2FC(O)OCH_3 + CH_4 \rightarrow CH_3C(O)OCH_3 + CH_3F \quad (R8)$$

$$CH_2FC(O)OCH_3 + CH_3Cl \rightarrow CH_3C(O)OCH_3 + CH_2FCl \quad (R9)$$

The procedure involved during the evaluation of heat of formation using the isodesmic method is described here in brief. Optimization and frequency calculation of all the species involved in the isodesmic reactions R7–R9 were obtained at the MPWB1K/6-31+G(d,p) level. Energy values were further refined by making single-point energy calculation at the G2(MP2) level. At first reaction enthalpies $\Delta_rH^\circ_{298}$ of the isodesmic reactions R7–R9 were calculated by taking the total energy at the MPWB1K/6-31+G(d,p) and G2(MP2) levels of theory. In both cases the thermal correction to enthalpy obtained at the MPWB1K/6-31+G(d,p) level was used. Since reaction enthalpy corresponds to the difference of the enthalpy of formation between the products and the reactants, the heat of formation of a particular species can easily be calculated by combining the reaction enthalpy with the known enthalpies of formation of the reference compounds involved in the isodesmic reaction schemes. The experimental $\Delta_fH^\circ_{298}$ values for CH_4 (−17.89 kcal mol^{-1}), CH_3CH_3 (−20.04 kcal mol^{-1}), CH_3COCH_3 (−52.23 kcal mol^{-1}), CH_3OCH_3 (−43.9 kcal mol^{-1}), CH_3Cl (−19.59 kcal mol^{-1}), $CH_3C(O)OCH_3$ (−98.0 kcal mol^{-1}), and CH_2F_2 (−107.71 kcal mol^{-1}) were taken from ref 21, and that of CH_2FCl (−63.2 kcal mol^{-1}) was taken from ref 45 and that of CH_3F (−55.97 kcal mol^{-1}) from ref 46. The obtained enthalpies of formation at two different levels of theory are listed in Table 2. Results show that the heats of formation calculated at both levels yield consistent values. First $\Delta_fH^\circ_{298}$ values for both conformers of MFA are obtained from the average of results obtained from the three isodesmic reactions R7–R9. Then the $\Delta_fH^\circ_{298}$ value for MFA is determined using statistical weight factor and $\Delta_fH^\circ_{298}$ values for both conformers SC1 and SC2. The $\Delta_fH^\circ_{298}$ values of radicals $CH_2FC(O)OC^\bullet H_2$ and $C^\bullet HFC(O)OCH_3$ are calculated utilizing $\Delta_rH^\circ_{298}$ values for reactions R1–R2, $\Delta_fH^\circ_{298}$ value for MFA, and the experimental $\Delta_fH^\circ_{298}$ values for H_2O (−57.8 kcal mol^{-1}) and OH (8.93 kcal mol^{-1}) radical.[47] The $\Delta_fH^\circ_{298}$ for $CH_2FC(O)OCH_3$, $CH_2FC(O)OC^\bullet H_2$, and $C^\bullet HFC(O)OCH_3$ radicals calculated from G2(MP2) results are −136.70, −87.89, and −86.50 kcal mol^{-1}, respectively. A detailed literature survey reveals that no experimental data are available for comparison. Table S3 of Supporting Information lists the D°_{298} values for $-CH_3$ and $-CH_2F$ sites of MFA molecule. The D°_{298} values for the $-CH_3$ and $-CH_2F$ sites of MFA amounting to 100.96 and 102.44 kcal mol^{-1}, respectively, at G2(MP2) are seen to be basically good with the literature values of 100.80 and 102.0 kcal mol^{-1} in a similar species $CH_2FCF_2OCH_3$ reported by Wang et al.[48] Since D°_{298} of $-CH_3$ is lower than that of the $-CH_2F$ sites, hydrogen abstraction from the $-CH_3$ site will be more favorable, which is in accord with barrier height calculations.

Table 2. Enthalpies of Formation ($\Delta_fH^\circ_{298}$) for Species Calculated from the Isodesmic Reactions[a]

species	isodesmic reaction schemes	G2(MP2)	MPWB1K
SC1	R3	−137.49	−138.50
	R4	−136.15	135.97
	R5	−136.86	−137.16
	av	−136.83	−137.21
SC2	R3	−137.17	−138.29
	R4	−135.83	−135.76
	R5	−136.54	−136.96
	av	−136.51	−137.00
$CH_2FC(O)OCH_3$	wt-av value	−136.70	−137.12
$CH_2FC(O)OC^\bullet H_2$		−87.89	−85.61
$C^\bullet HFC(O)OCH_3$		−86.50	−85.0

[a]All values are in kcal mol^{-1}.

dx.doi.org/10.1021/jp5032042 | J. Phys. Chem. A 2014, 118, 8779–8786

Rate Constants. The rate constants for title reactions are evaluated using the conventional transition state theory (TST)[49] equation:

$$k = \sigma\kappa \frac{k_B T}{h} \frac{Q^{\ddagger}_{TS}}{Q_R} \exp \frac{-\Delta E}{RT} \quad (2)$$

where σ is the reaction path degeneracy accounting for the number of equivalent reaction paths and κ is the tunneling correction. The σ value for R1 and R2 is taken as 2 because three H atoms present in the $-CH_3$ group are not equivalent. ΔE is the barrier height; k_B and h are the Boltzmann and Planck constants. R represents the universal gas constant. $Q^{\ddagger}_{TS}$ and Q_R are the total partition function (per unit volume) for the transition states and reactants, respectively, and obtained from the vibrational frequency calculation performed at the MPWB1K/6-31+G(d,p) level. In the calculation of electronic partition function for the OH radical, the excited state of the OH radical is included, with a 140 cm^{-1} splitting due to spin−orbit coupling. The tunneling correction factor κ is defined as the ratio of the quantum mechanical to the classical mechanical barrier crossing rate. The tunneling correction κ was estimated by using the Eckart's unsymmetric barrier method.[50,51] The tunneling correction factors over the temperature range of 250−450 K are given in the Supporting Information (Table S4). The hindered-rotor approximation of Chuang and Truhlar[52] was used for calculating the partition function of lower vibration modes. Using Truhlar's procedure[53] the q^{HIN}/q^{HO} ratio was found to be in the range of 0.78 to 0.99. We have followed the procedure proposed by Singleton and Cvetanovoic[54] for taking into consideration the effect of pre- and postreactive complex on reaction kinetics.

Since MFA possesses two conformers (SC1 and SC2) close in energy and each of their reactions with OH radicals passes through two different channels, the rate coefficient values for two conformers (k_{SC1} and k_{SC2}) are obtained by adding up the rate coefficients for the two channels originating from each conformer: $k_{SC1} = k_{TSa1} + k_{TSb1} + k_{TS21}$ and $k_{SC2} = k_{TSa2} + k_{TSb2} + k_{TS22}$.

The k_{OH} is computed by Boltzmann equation[41] using the rate constants for both conformers (k_{SC1} and k_{SC2}). The results obtained at the G2(MP2) level are summarized in Table S5 in Supporting Information. At 298 K, our calculated k_{OH} value using G2(MP2) barrier heights is 2.44×10^{-13} cm^3 $molecule^{-1}$ s^{-1}, which underestimates the value reported by Smith et al.[55] as $(3.85 \pm 0.349) \times 10^{-13}$ cm^3 $molecule^{-1}$ s^{-1}) for $CH_3C(O)OCH_3$ and higher than the value of $(1.48 \pm 0.34) \times 10^{-13}$ cm^3 $molecule^{-1}$ s^{-1} for $CF_2HC(O)OCH_3$ reported by Blanco and Teruel.[14] This is due to substitution of the more electronegative fluorine atom, which makes the adjacent carbon positively charged. Thus, C−H bond strengths enhance and, in turn, the rate constant for hydrogen abstraction reactions also increases. This can also be endorsed to the more negative inductive effect associated with $-CH_2F$ group. The temperature variations of k_{OH} at the G2(MP2) level are shown in Figure 2. In order to make a comparison, we summarized the rate constant of FESs with OH radicals in Table 3. The results given in Table 3 reveal that the higher the number of the hydrogen atoms in FESs, the greater the reaction rate with OH radicals. This is in accord with the observation reported by Blanco and Teruel.[14] Due to scarcity of rate constant in higher temperatures, rate constants for the title reaction are fitted in an Arrhenius equation as follows: $k = 8.79 \times 10^{-13} \exp[(-377.27 \pm 64)/T]$ cm^3 $molecule^{-1}$ s^{-1} over the range 250−450 K.

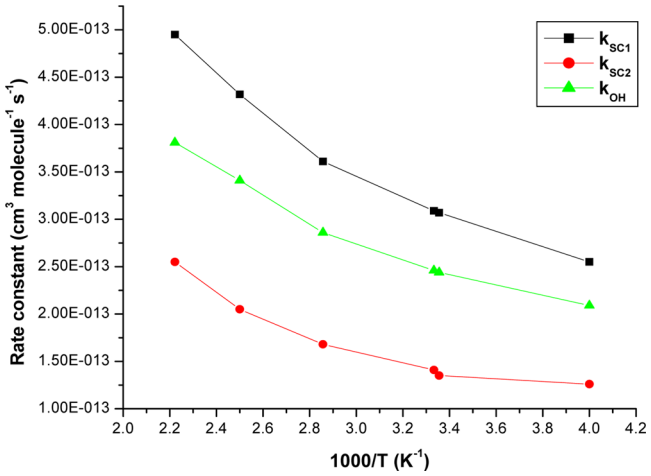

Figure 2. Rate constants for hydrogen abstraction reactions of two conformers (SC1 and SC2) of MFA and total rate constant (k_{OH}) for the MFA + OH reactions at the G2(MP2) level.

Table 3. Comparison of the Rate Constant Values for the Reaction of OH Radicals with Fluoroacetates and Acetates at 298 K

species	k_{OH} (cm^3 $molecule^{-1}$ s^{-1})	refs
$CF_3C(O)OCH_3$	$(4.97 \pm 1.04) \times 10^{-14}$	Blanco and Teruel[16]
	5.50×10^{-14}	Chakrabatty et al.[20]
$CF_2HC(O)OCH_3$	$(1.48 \pm 0.34) \times 10^{-13}$	Blanco and Teruel[16]
	1.38×10^{-13}	Singh et al.[24]
$CH_2FC(O)OCH_3$	2.44×10^{-13}	this work
$CH_3C(O)OCH_3$	$(3.85 \pm 0.349) \times 10^{-13}$	Smith et al.[54]

Atmospheric Implications. The atmospheric sink of any compound depends on various processes like photolysis, wet and dry deposition, and reaction with atmospheric oxidants such as OH radicals, Cl atoms, and O_3 and NO_3 radicals. Previous reports[17,23,56] reveal that photolysis and reactions with NO_3 and O_3 radicals are to be unimportant for saturated esters. The hydrophobic nature and volatility of esters will render wet deposition and dry deposition an unlikely removal process. A rate coefficient for the gas-phase reaction of MFA with Cl atoms is not known. Thus, atmospheric lifetime (τ_{eff}) of MFA is mainly controlled by OH-initiated hydrogen abstraction. Then the OH-driven atmospheric lifetime (τ_{eff}) is calculated using the relationship $(\tau_{eff}) = (k_{OH} \times [OH])^{-1}$, with $k_{OH} = 2.44 \times 10^{-13}$ cm^3 $molecule^{-1}$ s^{-1} and [OH] concentrations[57] of 2.0×10^6 molecules cm^{-3}. The calculated atmospheric lifetime is 24 days with respect to reaction with OH radical.

Fate of Alkoxy Radical. Theoretical calculations at the G2(MP2)//MPWB1K/6-31+G(d,p) level of theory were carried out in order to explore the nature of the reaction mechanism for the unimolecular decomposition of $CH_2FC(O)OCH_2O^{\bullet}$ in the gas phase. The optimized geometries and structural parameters of reactant and transition states for reaction channels (R3−R6) at the MPWB1K level are depicted in Figure 1. The thermochemical data calculated at the G2(MP2) and MPWB1K/6-31+G(d,p) levels are summarized in Table S6 in the Supporting Information. Transition vectors for all the transition states TS3, TS4, TS5, and TS6 were obtained at 979i, 1959i, 321i, and 1057i cm^{-1}, respectively as recorded in Table S7 in the Supporting Information. The α-

dx.doi.org/10.1021/jp5032042 | J. Phys. Chem. A 2014, 118, 8779−8786

ester rearrangement pathway (R3) involves a five-membered cyclic transition state TS3, which includes two bond cleavages (C3−H1 and C3−O2) and formation of an O1−H1 bond. The hydrogen atom approaches the carbonyl oxygen O1 with a distance of 1.280 Å. The C3−H1and C3−O2 bonds are found to be elongated by 21.25 to 24.24%, whereas the moving H atom maintains the distance of 1.250 Å for C2−O1 and C2−O2 bonds. This process is calculated to be exothermic and exergonic ($\Delta G < 0$). The G2(MP2) calculated energy barrier for TS3 is found to be 14.14 kcal mol^{-1} whereas the MPWB1K/6-31+G(d,p) result amounts to 16.41 kcal mol^{-1} as recorded in Table 4. A close look at the optimized structure

Table 4. Calculated Barrier Heights for Transition States Involved in Thermal Decomposition of $CH_2FC(O)OCH_2O^•$ Radical at Various Levels of Theory[a]

reaction channels	G2(MP2)	MPWB1K/6-31+G(d,p)	B3LYP/6-311G(2df,2p)	B3LYP/6-31G(d,p)
TS3 (α-ester rearrangement)	14.14	16.41	7.45	8.34
TS4 (reaction with O_2)	11.86	13.53	5.73	4.43
TS5 (C−O bond scission)	19.96	28.44	15.88	16.62
TS6 (C−H bond scission)	18.56	25.85	20.73	22.59

[a]All values are in kcal mol^{-1}.

of TS4 reveals that the breaking C3−H1 bond is lengthened from 1.096 to 1.275 Å (16.33%) whereas the forming H1−O4 bond is elongated by 41.7% during transition. It is obvious from Table S6 in the Supporting Information that the oxidative pathway is significantly exothermic and exergonic and thus thermodynamically more facile. This process is accompanied by the energy barriers of 11.86 and 13.53 kcal mol^{-1} at the G2(MP2) and MPWB1K/6-31+G(d,p) levels, respectively. The transition state TS5 corresponding to the C3−O2 bond scission (channel R5) leading to formaldehyde (CH_2O) and $CH_2FC(O)O$ shows a substantial elongation (45.73%) in the rupturing C3−O2 bond and a shortening of the C3−O3 bond from 1.323 to 1.224 (7.48%). Similarly, in the optimized geometry of TS6, the breaking C−H bond is found to be elongated by almost 60%. It is obvious from Table S6 in the Supporting Information that the thermal decomposition pathways (R5 and R6) are accompanied by an endothermicity of 17.93 and 11.04 kcal mol^{-1}, respectively, at the G2(MP2) level with a positive free energy change and thus are thermodynamically less probable. The results recorded in Table 4 suggest that the barriers of TS5 and TS6 are significantly higher than those of TS3 and TS4. Based on energetics and thermochemical data, it may be concluded that thermal decomposition pathways (C−O and C−H bond scissions) leading to the formation of formaldehyde do not compete with α-ester rearrangement and oxidative pathways. Literature survey reveals that the reactivity of alkoxy radical considered during the present work is similar to an early study of Ferenac et al.[29] for $CH_3C(O)OCH_2O^•$ radical. The computed barrier heights for α-ester rearrangement as 8.34 and 7.45 kcal mol^{-1} agree well with those of 8.0 and 7.2 kcal mol^{-1}, respectively, for $CH_2FC(O)OCH_2O^•$ radical at the B3LYP/6-31G(d,p) and B3LYP/6-311G(2df,2p) levels reported by Ferenac et al.[29] The barrier heights for oxidation reaction at B3LYP levels are found to be 4.43 and 5.73 kcal mol^{-1}, respectively. Thus, the barrier heights for oxidative pathways are lower than for other pathways and the dominance of this pathway is envisioned. This is in line with the fact of the high yield of $CF_2HC(O)OCHO$ assigned by Blanco et al.[22] for a similar fluoroester MDFA ($CF_2HC(O)OCH_3$). The rate constants for competitive reaction channels (R3 and R4) are calculated using ab initio data. The calculated rate constant is found to be 1.09×10^{-17} s^{-1} and 2.32×10^{-20} cm^{-3} molecule^{-1} s^{-1}, respectively, for reaction channels R3 and R5 at 298 K. The associated A factors for reaction channels R3 and R5 come out to be 2.48×10^{-7} s^{-1} and 1.12×10^{-11} cm^{-3} molecule^{-1} s^{-1} at the G2(MP2)//MPWB1K level of theory.

CONCLUSIONS

In the present work, a systematic investigation is performed on OH-initiated oxidation mechanism of $CH_2FC(O)OCH_3$ using a high-level ab initio method. The potential energy surface information is obtained at the G2(MP2)//MPWB1K/6-31+G(d,p) level of theory. The reaction may proceed via an indirect mechanism. The calculated total rate constant at 298 K is found to be 2.44×10^{-13} cm^3 molecule^{-1} s^{-1} using G2(MP2) results. For rate constants at higher temperatures, a model equation $k = 8.79 \times 10^{-13} \exp[(-377.27 \pm 64)/T]$ cm^3 molecule^{-1} s^{-1} has been derived. Based on energetics and kinetic calculations, it is shown that the attack of OH radicals occurs predominately at the $-CH_3$ site. This is further ascertained by the calculated C−H bond dissociation energy of the MFA molecule. The $\Delta_f H^\circ_{298}$ values for MFA, $CH_2FC(O)OC^•H_2$, and $C^•HFC(O)OCH_3$ radical are estimated to be −136.70, −87.89, and −86.50 kcal mol^{-1}, respectively. The OH-driven lifetime of MFA was estimated to be around 24 days. Based on mechanistic studies, our results suggest that an oxidation pathway is likely to be the dominant fate, whereas thermal decomposition pathways (C−O and C−H bond scissions) do not compete with other pathways in the consumption of $CH_2FC(O)OCH_2O^•$ radical. The kinetic parameters for the α-ester rearrangement and oxidative pathways are estimated and found to be 1.09×10^{-17} s^{-1} and 2.32×10^{-20} cm^3 molecule^{-1} s^{-1}, respectively, at 298 K.

ASSOCIATED CONTENT

Supporting Information

Harmonic vibrational frequencies, relative energies and optimized geometries of reactant complexes, product complexes, products, and transition states at the MPWB1K/6-31+G(d,p) level of theory. This material is available free of charge via the Internet at http://pubs.acs.org.

AUTHOR INFORMATION

Corresponding Authors

*(B.K.M.) Tel: +91 3712267008. Fax: +91 3712267005. E-mail: bhupesh@tezu.ernet.in; bhupesh_chem@rediffmail.com.
*(R.C.D.) Tel: +91 3712267008. Fax: +91 3712267005. E-mail: ramesh@tezu.ernet.in.

Notes

The authors declare no competing financial interest.

ACKNOWLEDGMENTS

The authors acknowledge financial support from the Department of Science and Technology, New Delhi, in the form of a project (SR/NM.NS-1023/2011(G)). B.K.M. is thankful to University Grants Commission, New Delhi, for providing

financial support in the form of UGC-Dr. D. S. Kothari fellowship. We are also thankful to the reviewers for their valuable comments to improve the quality of the manuscript.

REFERENCES

(1) Molina, M. J.; Rowland, F. S. Stratospheric sink for chlorofluoromethanes: chlorine atom-catalysed destruction of ozone. *Nature* **1974**, *249*, 810−812.
(2) Farman, J. D.; Gardiner, B. G.; Shanklin, J. D. Large losses of total ozone in Antarctica reveal seasonal ClO_x/NO_x interaction. *Nature* **1985**, *315*, 207−210.
(3) Powell, R. L. CFC Phase-out: Have we met the challenge? *J. Fluorine Chem.* **2002**, *114*, 237−250.
(4) Sekiya, A.; Misaki, S. The potential of hydrofluoroethers to replace CFCs, HCFCs and PFCs. *J. Fluorine Chem.* **2000**, *101*, 215−221.
(5) Ravishankara, A. R.; Turnipseed, A. A.; Jensen, N. R.; Barone, S.; Mills, M.; Howark, C. J.; Solomon, S. Do hydrofluorocarbons destroy stratospheric ozone? *Science* **1994**, *263*, 71−75.
(6) Nohara, K.; Toma, M.; Kutsuna, S.; Takeuchi, K.; Ibusuki, T. Cl atom-initiated oxidation of three homologous methyl perfluoroalkyl ethers. *Environ. Sci. Technol.* **2001**, *35* (1), 114−120.
(7) Oyaro, N.; Sellevag, S. R.; Nielsen, C. J. Study of the OH and Cl-initiated oxidation, IR absorption cross-section, radiative forcing and global warming potential of four C4-Hydrofluoroethers. *Environ. Sci. Technol.* **2004**, *38*, 5567−5576.
(8) Christensen, L. K.; Sehested, J.; Nielsen, O. J.; Bilde, M.; Wallington, T. J.; Guschin, A.; Molina, L. T.; Molina, M. J. Atmospheric chemistry of HFE-7200 ($C_4F_9OC_2H_5$): reaction with OH radicals and fate of $C_4F_9OCH_2CH_2O(\bullet)$ and $C_4F_9OCHO(\bullet)CH_3$ radicals. *J. Phys. Chem. A* **1998**, *102*, 4839−4845.
(9) Wallington, T. J.; Schneider, W. F.; Sehested, J.; Bilde, M.; Platz, J.; Nielsen, O. J.; Christensen, L. K.; Molina, M. J.; Molina, L. T.; Wooldridge, P. W. Atmospheric chemistry of HFE-7100 ($C_4F_9OCH_3$): reaction with OH radicals, UV spectra and kinetic data for $C_4F_9OCH_2$ and $C_4F_9OCH_2O_2$ radicals and the atmospheric fate of $C_4F_9OCH_2O$ radicals. *J. Phys. Chem. A* **1997**, *101*, 8264−8274.
(10) Ninomiya, Y.; Kawasaki, M.; Guschin, A.; Molina, L. T.; Molina, M. J.; Wallington, T. J. Atmospheric chemistry of *n*-$C_3F_7OCH_3$: reaction with OH radicals and Cl atoms and atmospheric fate of *n*-$C_3F_7OCH_2O$ radicals. *Environ. Sci. Technol.* **2000**, *34* (14), 2973−2978.
(11) Chen, L.; Kutsuna, S.; Tokuhashi, K.; Sekiya, A. Kinetics of the gas-phase reaction of $CF_3OC(O)H$ with OH radicals at 242−328 K. *Int. J. Chem. Kinet.* **2004**, *36* (6), 337−344.
(12) Blanco, M. B.; Barnes, I.; Teruel, M. A. Product distribution in the Cl-initiated photooxidation of $CF_3C(O)OCH_2CF_3$. *J. Phys. Org. Chem.* **2010**, *23*, 950−954.
(13) Blanco, M. B.; Bejan, I.; Barnes, I.; Wiesen, P.; Teruel, M. Atmospheric photooxidation of fluoroacetates as a source of fluorocarboxylic acids. *Environ. Sci. Technol.* **2010**, *44* (7), 354−2359.
(14) Blanco, M. B.; Teruel, M. A. Atmospheric degradation of fluoroesters (FESs): gas phase reactivity study towards OH radicals at 298 K. *Atmos. Environ.* **2007**, *41*, 7330−7338.
(15) Blanco, M. B.; Bejan, I.; Barnes, I.; Wiesen, P.; Teruel, M. Kinetics of the reactions of chlorine atoms with selected fluoroacetates at atmospheric pressure and 298 K. *Chem. Phys. Lett.* **2008**, *453*, 18−23.
(16) Blanco, M. B.; Teruel, M. A. Rate constants of the reactions of $CF_2ClC(O)OCH_3$ and $CF_2ClC(O)OCH_2CH_3$ with OH radicals and Cl atoms at atmospheric pressure. *Chem. Phys. Lett.* **2007**, *441*, 1−6.
(17) Blanco, M. B.; Rivela, C.; Teruel, M. A. Tropospheric degradation of 2,2,2 trifluoroethyl butyrate: Kinetic study of their reactions with OH radicals and Cl atoms at 298 K. *Chem. Phys. Lett.* **2013**, *578*, 33−37.
(18) Chakrabartty, A. K.; Mishra, B. K.; Bhattacharjee, D.; Deka, R. C. Mechanistic and kinetics study of the gas phase reactions of methyltrifluoroacetate with OH radical and Cl atom. *Mol. Phys.* **2013**, *111*, 860−867.
(19) Gour, N. K.; Deka, R. C.; Singh, H. J.; Mishra, B. K. A Computational perspective on mechanism and kinetics of the reactions of $CF_3C(O)OCH_2CF_3$ with OH radicals and Cl atoms at 298 K. *J. Fluorine Chem.* **2014**, *160*, 64−73.
(20) Mishra, B. K.; Chakrabartty, A. K.; Deka, R. C. A theoretical investigation on the kinetics and reactivity of the gas-phase reactions of ethyl chlorodifluoroacetate with OH radical and Cl atom at 298 K. *Struct. Chem.* **2014**, *25*, 463−470.
(21) Mishra, B. K.; Chakrabartty, A. K.; Deka, R. C. Theoretical investigation of the gas phase reactions of $CF_2ClC(O)OCH_3$ with the hydroxyl radical and the chlorine atom at 298 K. *J. Mol. Model.* **2013**, *19*, 3263−3270.
(22) Singh, H. J.; Tiwari, L.; Rao, P. K. Computational study on the kinetics of OH initiated oxidation of methyl difluoroacetate ($CF_2HCOOCH_3$). *Mol. Phys.* **2014**, *112*, 1892−1898.
(23) Bravo, I.; Díaz-de-Mera, Y.; Aranda, A.; Moreno, E.; Nutt, D. R.; Marston, G. Radiative efficiencies for fluorinated esters: indirect global warming potentials of hydrofluoroethers. *Phys. Chem. Chem. Phys.* **2011**, *13*, 17185−17193.
(24) Foss, G. L. The toxicology and pharmacology of methyl fluoroacetate (MFA) in animals, with some notes on experimental therapy. *Br. J. Pharmacol.* **1948**, *3*, 118−127.
(25) Urata, S.; Takada, A.; Uchimaru, T.; Chandra, A. K. Rate constants estimation for the reaction of hydrofluorocarbons and hydrofluoroethers with OH radicals. *Chem. Phys. Lett.* **2003**, *368*, 215−223.
(26) Singh, H. J.; Mishra, B. K. Ab-initio studies on the decomposition kinetics of CF_3OCF_2O radical. *J. Mol. Model.* **2011**, *17*, 415−422.
(27) Singh, H. J.; Mishra, B. K.; Gour, N. K. Theoretical studies of decomposition kinetics of CF_3CCl_2O radical. *Theor. Chem. Acc.* **2010**, *125*, 57−64.
(28) Singh, H. J.; Mishra, B. K.; Rao, P. K. Computational study on the thermal decomposition and isomerization of the $CH_3OCF_2O\bullet$ radical. *Can. J. Chem.* **2012**, *90* (4), 403−409.
(29) Ferenac, M. A.; Davis, A. J.; Holloway, A. S.; Dibble, T. S. Isomerization and decomposition reactions of primary alkoxy radicals derived from oxygenated solvents. *J. Phys. Chem. A* **2003**, *107*, 63−72.
(30) Zhao, Y.; Truhlar, D. G. Hybrid meta density functional theory methods for thermochemistry, thermochemical kinetics, and noncovalent interactions: the MPW1B95 and MPWB1K models and comparative assessments for hydrogen bonding and van der Waals interactions. *J. Phys. Chem. A* **2004**, *108*, 6908−6918.
(31) Mishra, B. K. Theoretical investigation on the atmospheric fate of the $CF_3C(O)OCH(O)CF_3$ radical: alpha-ester rearrangement vs. oxidation. *RSC Adv.* **2014**, *4* (32), 16759−16764.
(32) Zeegers-Huyskens, T.; Lily, M.; Sutradhar, D.; Chandra, A. K. Theoretical study of the O···Cl interaction in fluorinated dimethyl ethers complexed with a Cl atom: is it through a two-center-three-electron bond? *J. Phys. Chem. A* **2013**, *117*, 8010−8016.
(33) Devi, Kh. J.; Chandra, A. K. Theoretical investigation of the gas-phase reactions of $(CF_3)_2CHOCH_3$ with OH radical. *Chem. Phys. Lett.* **2011**, *502*, 23−28.
(34) Chakrabatty, A. K.; Mishra, B. K.; Bhattacharjee, D.; Deka, R. C. Theoretical study on the kinetics and branching ratios of the gas phase reactions of 4,4,4-Trifluorobutanal (TFB) with OH radical in the temperature range of 250−400 K and atmospheric pressure. *J. Fluorine Chem.* **2013**, *154*, 60−66.
(35) Gonzalez, C.; Schlegel, H. B. An improved algorithm for reaction path following: higher-order implicit algorithms. *J. Chem. Phys.* **1989**, *90*, 2154−2161.
(36) Curtiss, L. A.; Raghavachari, K.; Pople, J. A. Gaussian-2 theory using reduced Møller Plesset orders. *J. Chem. Phys.* **1993**, *98*, 1293−1297.
(37) Mishra, B. K.; Chakrabatty, A. K.; Bhattacharjee, D.; Deka, R. C. Theoretical investigation on unimolecular decomposition of malonic

acid: a potential sink for ketene. *RSC Adv.* **2014**, *4* (72), 38034−38039.
(38) Mishra, B. K.; Lily, M.; Deka, R. C.; Chandra, A. K. Theoretical investigation on gas−phase reaction of $CF_3CH_2OCH_3$ with OH radicals and fate of alkoxy radicals ($CF_3CH(O\bullet)OCH_3$/$CF_3CH_2OCH_2O\bullet$). *J. Mol. Graphics Model.* **2014**, *50*, 90−99.
(39) Deka, R. C.; Mishra, B. K. A theoretical investigation on the kinetics, mechanism and thermochemistry of gas-phase reactions of methyl acetate with chlorine atoms at 298 K. *Chem. Phys. Lett.* **2014**, *595*−*596*, 43−47.
(40) Frisch, M. J.; Trucks, G. W.; Schlegel, H. B.; Scuseria, G. E.; Robb, M. A.; Cheeseman, J. R.; Scalmani, G.; Barone, V.; Mennucci, B.; Petersson, G. A.; et al. *Gaussian 09, Revision B.01*; Gaussian, Inc.: Wallingford, CT, 2010.
(41) McQuarrie, D. A. *Statistical mechanics*; VIVA: New Delhi, 2003.
(42) Abraham, R. J.; Tormenab, C. F.; Rittner, R. Conformational analysis. Part 35. NMR, solvation and theoretical investigation of rotational isomerism in methyl fluoroacetate and methyl difluoroacetate. *J. Chem. Soc., Perkin Trans.* **2001**, *2*, 815−820.
(43) Sahnoun, R.; Fujimura, Y.; Kabuto, K.; Takeuchi, Y.; Noyori, R. Hyperconjugative electron-delocalization mechanism controlling the conformational preference of fluoroacetaldehyde and methyl fluoroacetates. *Bull. Chem. Soc. Jpn.* **2006**, *79*, 555−560.
(44) Yang, L.; Liu, J. Y.; Li, Z. S. Theoretical studies of the reaction of hydroxyl radical with methyl acetate. *J. Phys. Chem. A* **2008**, *112*, 6364−6372.
(45) Roux, E. T.; Paddison, S. Bond dissociation energies and radical heats of formation in CH_3Cl, CH_2Cl_2, CH_3Br, CH_2Br_2, CH_2FCl, and $CHFCl_2$. *Int. J. Chem. Kinet.* **1987**, *19*, 15−24.
(46) Zhu, P.; Ai, L. L.; Wang, H.; Liu, J. Y. Theoretical studies on mechanism and kinetics of the hydrogen-abstraction reaction of $CF_2HCOOCH_3$ with OH radicals. *Comput. Theor. Chem.* **2014**, *1029*, 91−98.
(47) Lide, D. R. *CRC Handbook of Chemistry and Physics*, 80th ed.; CRC Press: New York, 1999.
(48) Wang, L.; Zhao, J.; He, H.; Zhang, J. Theoretical studies on the reactions of $CHF_2CF_2OCH_3$/$CH_2FCF_2OCH_3$ with OH radicals. *J. Fluorine Chem.* **2013**, *149*, 72−81.
(49) Laidler, K. J. *Chemical kinetics*, 3rd ed.; Pearson Education: Delhi, 2004.
(50) Brown, R. L. A method of calculating tunneling corrections for Eckart potential barriers. *J. Res. Natl. Bur. Stand.* **1981**, *86*, 357−359.
(51) Xiao, R.; Noerpel, M.; Luk, H. L.; Wei, Z.; Spinney, R. Thermodynamic and kinetic study of ibuprofen with hydroxyl radical: a density functional theory approaches. *Int. J. Quantum Chem.* **2014**, *114*, 74−83.
(52) Chuang, Y. Y.; Truhlar, D. G. Statistical thermodynamics of bond torsional modes. *J. Chem. Phys.* **2000**, *112*, 1221−1228.
(53) Truhlar, D. G. Simple approximation for the vibrational partition function of hindered internal rotation. *J. Comput. Chem.* **1991**, *12*, 266−270.
(54) Singleton, D. L.; Cvetonovoic, R. J. Temperature dependence of the reactions of oxygen atoms with olefins. *J. Am. Chem. Soc.* **1976**, *98*, 6812−6819.
(55) Smith, D. F.; McIver, C. D.; Kleindienst, T. E. Kinetics and mechanism of the atmospheric oxidation of tertiary amyl methyl ether. *Int. J. Chem. Kinet.* **1995**, *27*, 453−472.
(56) Spicer, C. W.; Chapman, E. G.; Finlayson-Pitts, B. J.; Plastridge, R. A.; Hubbe, J. M.; Fast, J. D.; Berkowitz, C. M. Unexpectedly high concentration of molecular chlorine in coastal air. *Nature* **1998**, *394*, 353−355.
(57) Hein, R.; Crutzen, P. J.; Heimann, M. An inverse modeling approach to investigate the global atmospheric methane cycle. *Global Biogeochem. Cycles* **1997**, *11*, 43−76.